

Supplementary Figures

S1. Expected number of successful *de novo* occurrences, \mathcal{S}

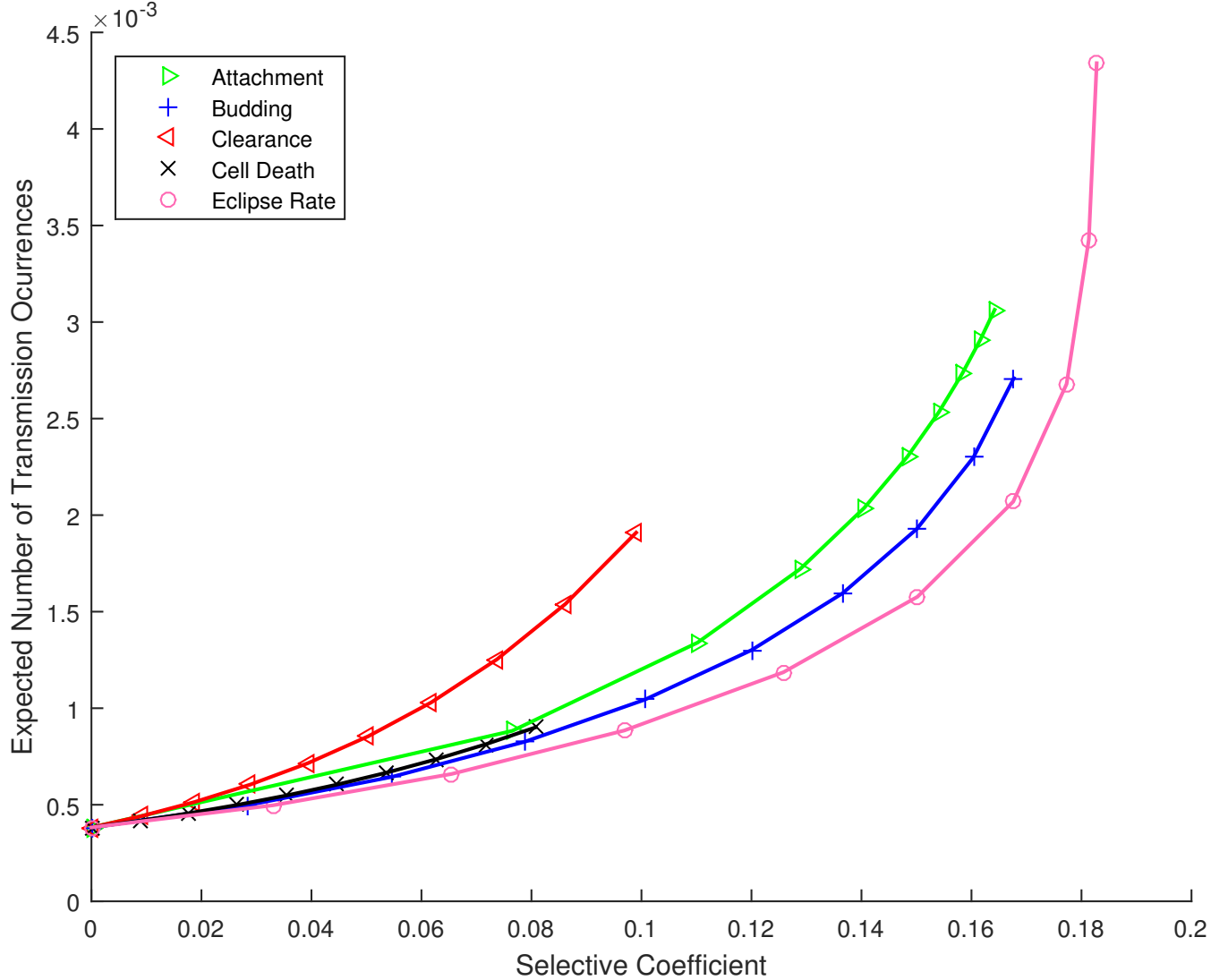


Figure S1: The number of times that a given mutation is expected to arise *de novo*, during a single infection time course, and produce a lineage that is transmitted to the next infected individual, \mathcal{S} , versus the selective coefficient. This quantity scales linearly with μ , the mutation rate per site per substitution.

S2. Expected number of transmitted mutant virions, \mathcal{N}

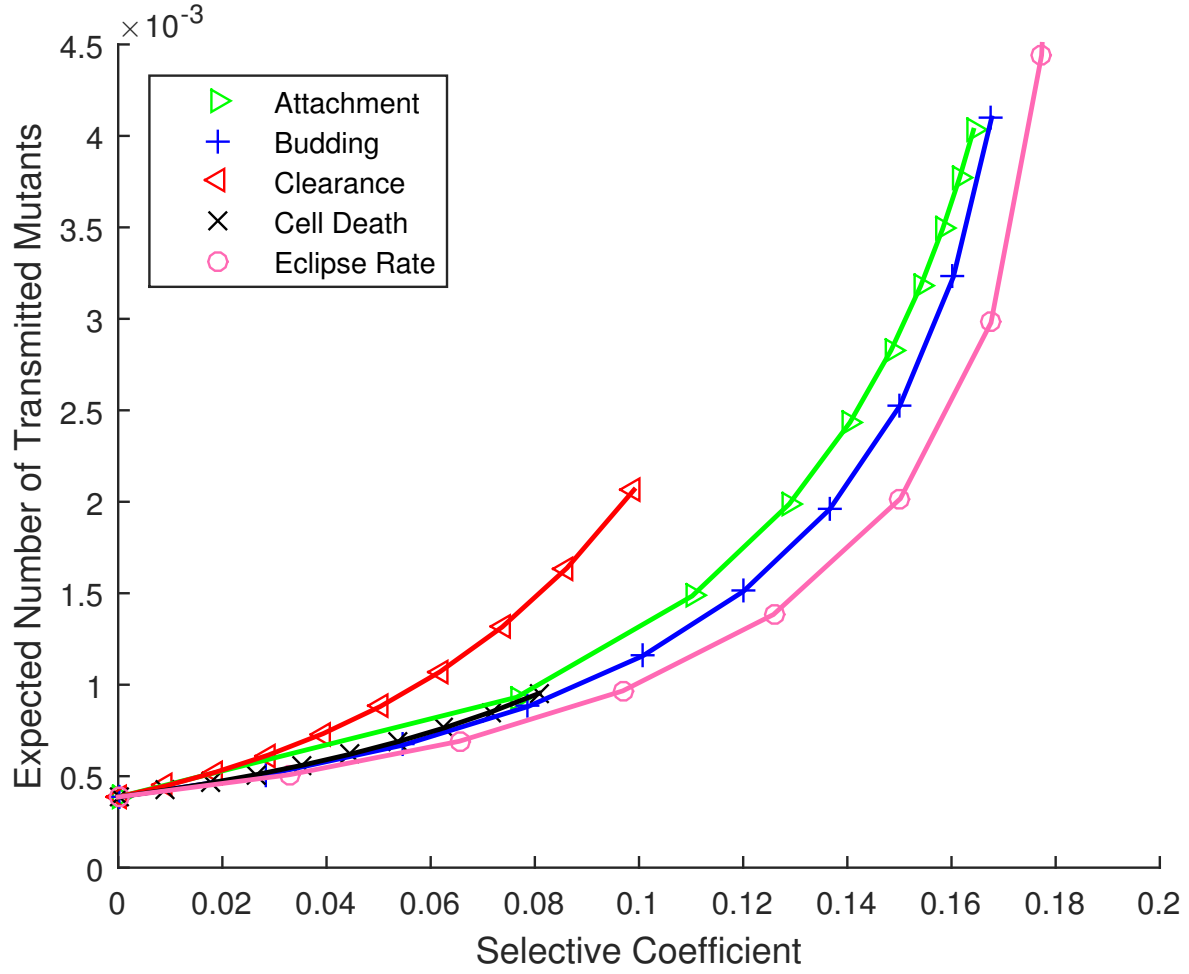


Figure S2: The expected number of virions transmitted to the recipient that have arisen *de novo* during a single infection time course in the donor (\mathcal{N} , as described in the Appendix), versus the selective coefficient.

S3. Effect of non-exponential cell lifetimes: Deterministic time course

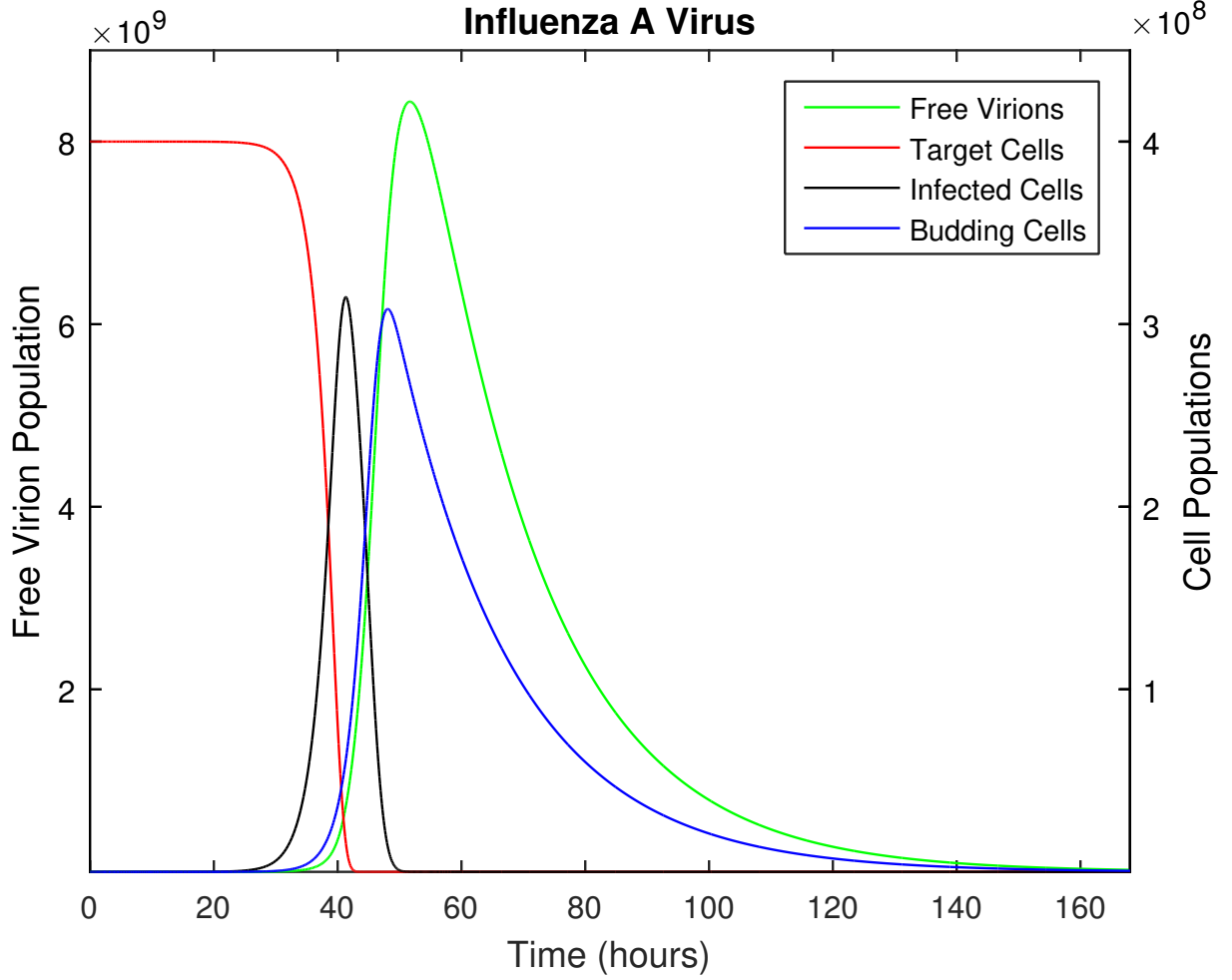


Figure S3: The time course of influenza A infection over the span of a week (168 hours). This figure is analogous to Figure 1, except that the cell death rate, D , has been set to zero during the eclipse stages, and increased during the budding phase such that the mean infected cell lifetime is unchanged. Other parameters as provided in Table 1. The infection time course is relatively insensitive to these changes in the distribution of infected cell lifetimes.

S4. Effect of non-exponential cell lifetimes: Transmission probability

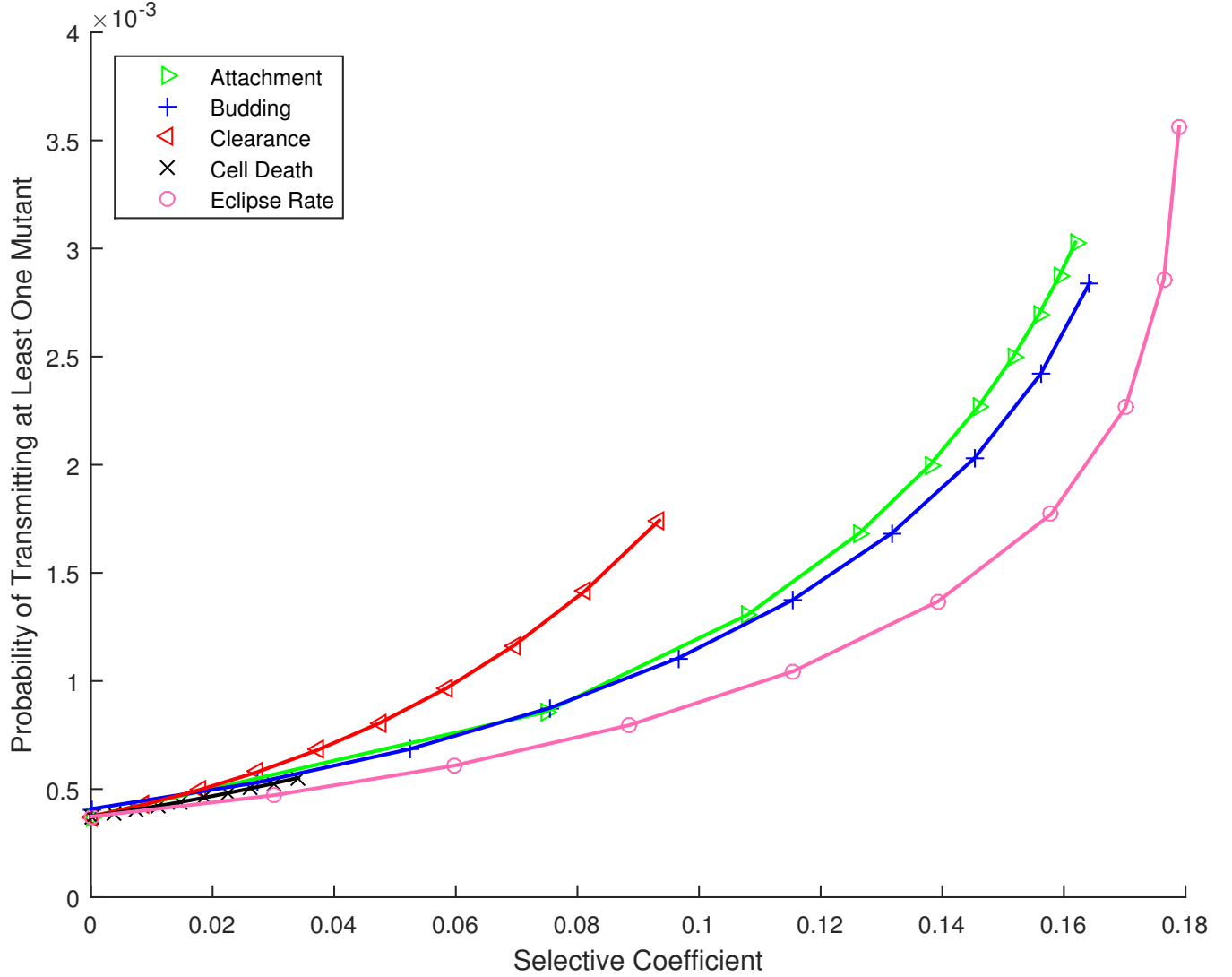


Figure S4: The probability that at least one copy of a specific *de novo* mutation arises during the infection time course and is passed to the next host, \mathcal{P} , versus the selective coefficient, s . This figure is analogous to Figure 2, except that the cell death rate, D , has been set to zero during the eclipse stages, and increased during the budding phase to yield the same mean infected cell lifetime. Other parameters as provided in Table 1. We find that the transmission of *de novo* mutations is insensitive to these changes in the distribution of infected cell lifetimes.

S5. Effect of available target cells: Deterministic time course

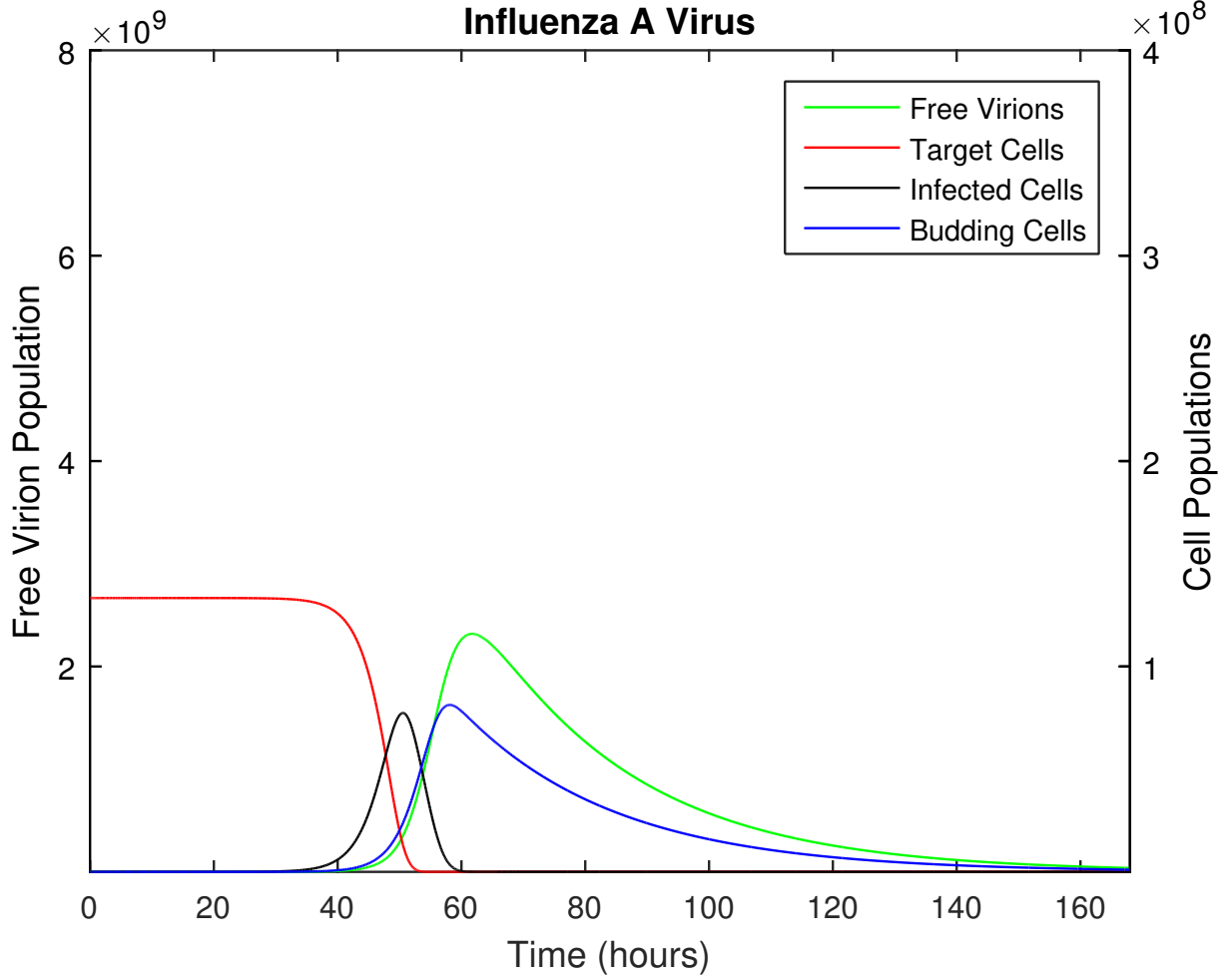


Figure S5: The time course of influenza A infection over the span of a week (168 hours). This figure is analogous to Figure 1, except that the initial target cell population, $y_T(0)$, has been reduced by a factor of 3. Although complete desquamation is the expected outcome of the infection, it is possible that spatial considerations might spare a fraction of the epithelial cells in the upper respiratory tract; we therefore included this case in sensitivity analysis. Other parameters as provided in Table 1. Comparing with Figure 1, the magnitude of the infection is scaled and the dynamics are slightly delayed. However this has little impact on the probability of transmission of a mutation (see Figure S6).

S6. Effect of number of available target cells: Transmission probability

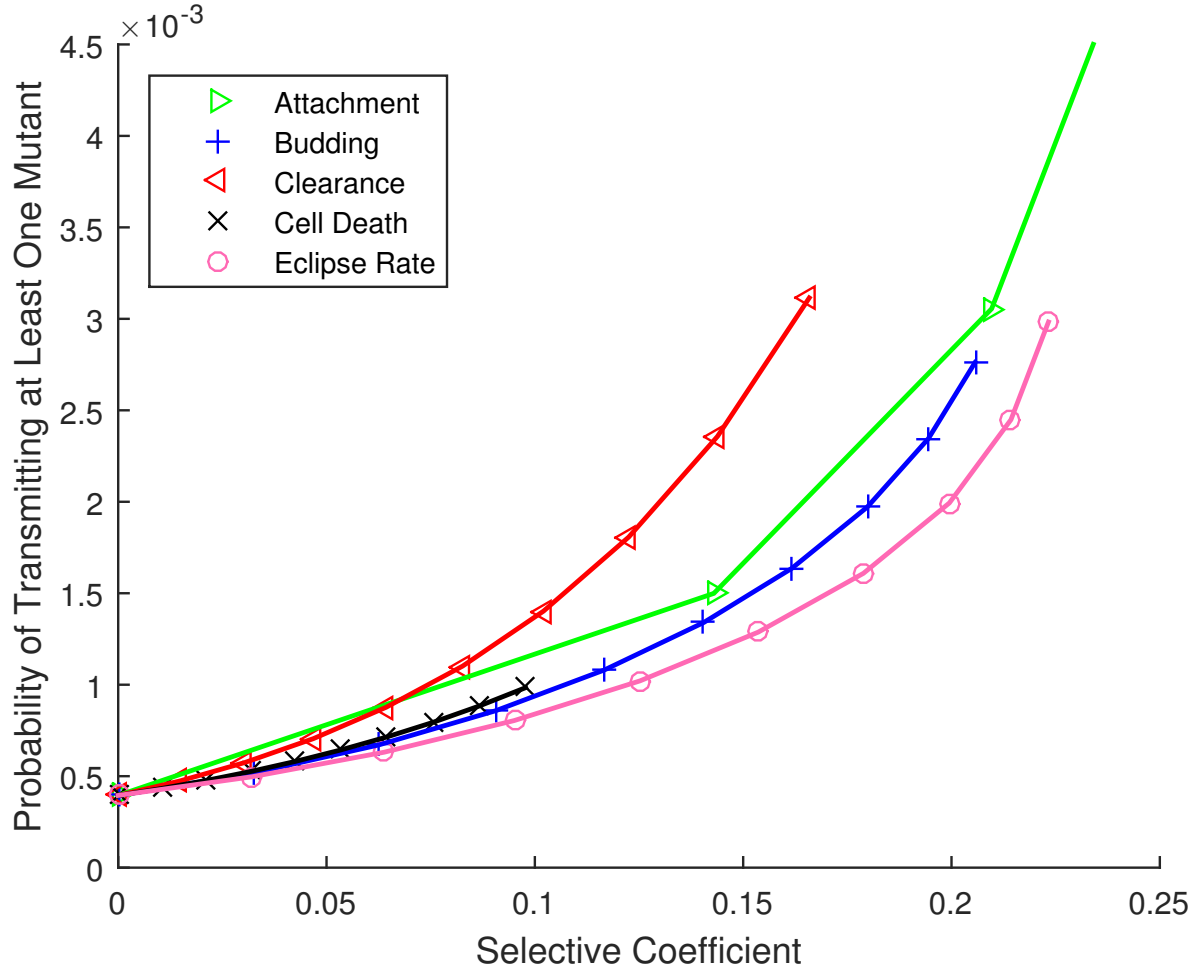


Figure S6: The probability that at least one copy of a specific *de novo* mutation arises during the infection time course and is passed to the next host, \mathcal{P} , versus the selective coefficient, s . This figure is analogous to Figure 2, except that the initial target cell population, $y_T(0)$, has been reduced by a factor of 3. Other parameters are as provided in Table 1. We find that the transmission of *de novo* mutations is insensitive to the initial number of available target cells.

S7. Effect of varying mutation rate

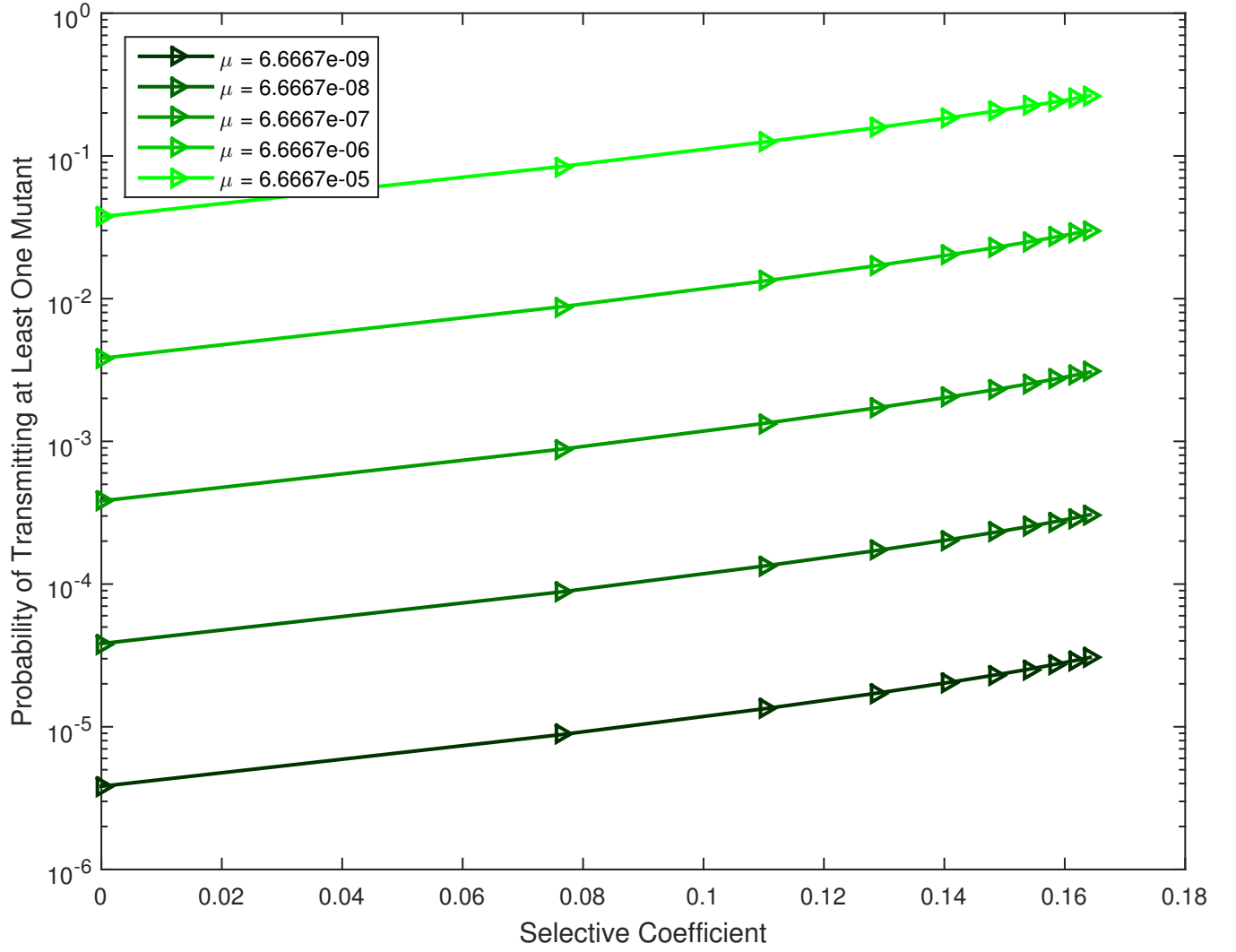


Figure S7: The effect of mutation rate on the probability of transmission. The probability that at least one copy of a *de novo* mutation is transmitted to the next host, \mathcal{P} , is plotted against the selective coefficient, for a mutation that increases the viral attachment rate. The mutation rate per replication event, μ , is varied. Other parameters as provided in Table 1.